

Mechanisms of Development of Photothermographic Media**

Susan E. Hill, Mark B. Mizen[†] and M. R. V. Sahyun[‡]

Medical Imaging Systems Division, 3M, St. Paul, Minnesota 55101

and Yuri E. Usanov

State Optical Institute "S. I. Vavilov," St. Petersburg, Russia

We have carried out an arrested development study on model thermally developed photographic materials (TDPM) based on silver carboxylates. From both TEM and x-ray diffraction analysis of the media at various stages of development, we infer that (1) during initiation of development small, spheroidal silver(0) particles form; (2) over the course of the development reaction, the number of silver(0) spheroids increases, but not their average size; (3) this process requires secondary nucleation of the silver(0) phase-forming reaction by an as-yet unestablished mechanism; and (4) above some threshold concentration, whose establishment corresponds to the onset of the continuation stage of development, these spheroids aggregate to form the light-absorbing particles comprising the TDPM image. Development kinetics of full-soap and half-soap systems were studied experimentally and by computer simulation to confirm the intermediacy of coordination complexes of silver ion and the role of carboxylic acid as the reaction product responsible for positive feedback in the development reaction. Our inferences are consistent with the Klosterboer–Rutledge model of development, but also imply that features of the recently proposed Usanov model are relevant as well.

Journal of Imaging Science and Technology 40: 568–575 (1996)

Historical Survey

Although thermally developed silver-based photoimaging media (TDPM) have been known for nearly 150 years,¹ the development of the modern products of commerce have their origin in silver carboxylate-based thermography copying paper and transparency film technology of the 1950s. Early on, the chemistry of the image-forming, thermal reaction between silver behenate and an organic reducing agent was characterized kinetically. The reaction was found to obey a pseudo-first-order rate law with an induction period:²

$$D = D\{1 - \exp[-k(t - t_i)]\}, \quad (1)$$

Original manuscript received June 3, 1996. Revised September 3, 1996.

*Presented in part at IS&T's 49th Annual Conference, May 1996, Minneapolis, Minnesota.

[†]This is Contribution No. 96-0167C from the Information, Imaging and Electronics Sector Laboratories, 3M.

[‡]Present address: Imation Corp., 1 Imation Place, Oakdale, MN 55128

[§]IS&T Fellow and Senior Member; present address: Department of Chemistry, University of Wisconsin, Eau Claire, WI 54702.

© 1996, IS&T—The Society for Imaging Science and Technology

where D is the image density achieved on development for time t , D is the maximum image density achieved on prolonged development, k is the pseudo-first-order rate constant, and t_i is the duration of the induction period.

Transmission electron microscopy (TEM) on a series of samples of such media in which the reaction was quenched at various stages (so-called arrested development) demonstrated that formation of very small metallic silver particles occurred during the induction period.² This result led to a search for photocatalytic processes that would generate such small silver particles as a consequence of irradiation. Both silver halides³ and a variety of n -type inorganic photoconductors⁴ were found to be useful in this regard. Photothermographic imaging technology thus has its roots in the mechanistic understanding of the development reaction.

In TDPM the reaction is thought to proceed in two stages,⁵ which we will call the initiation and continuation stages, following the usage of conventional photography. The first stage occurs primarily during the induction period, and it has been identified with formation of primarily filamentary silver,⁶ at least in silver halide-containing formulations. The continuation stage is responsible for most of the optical density of the image and is associated with formation of densely packed, spheroidal deposits of metallic silver, typically in the 500-Å size range.^{6,7}

Models

Three paradigms for the image-forming reaction in TDPM that have been proposed in the literature are more or less consistent with the above observations:

- Initially it was suggested⁸ that the continuation stage involves aggregation of silver atoms to form the spheroidal deposits. At temperatures of development such atomic silver species may result either from interaction of the silver carboxylate with a reducing agent or from thermal decomposition of the silver carboxylate itself.⁹ This model is consistent with the chemistry of some historical photothermographic processes¹⁰ that used silver carboxylate salts without an additional reducing agent. It is, essentially, a recapitulation of the original Ostwald model of photographic development,¹¹ which was long ago discredited for conventional photography.¹² Modern TDPM incorporate not only reducing agents, but also "toners," which are usually silver-complexing agents. In the context of this model, the function of silver complexing ligands is to stabilize the intermediate atomic silver species.⁸
- A mathematical model of the photothermographic response of TDPM was proposed by Rutledge and Klosterboer^{8,13} (KR model). The KR model is based on

analogy to solution physical development in conventional photography.¹⁴ Accordingly, each silver halide grain in the TDPM is surrounded by a volume of silver carboxylate, known as the "sphere of influence." Within the sphere of influence silver ions are capable of diffusing to the reactive latent image center, where they are deposited as metallic silver by reaction with the reducing agent. The growing silver(0) deposit thus acts as a catalytic nucleus for this new phase-forming reaction. The radius of the sphere of influence is determined by the diffusion range of the silver ions, and the function of silver complexing agents in the TDPM is accordingly to facilitate diffusion of silver ion to the latent image. Various predictions from the KR model have been confirmed in recent experimental studies.^{15,16}

Reactions according to the KR model should follow autocatalytic kinetics (or otherwise reflect positive feedback),¹⁴ but in practice it may be difficult (see below) to distinguish statistically between autocatalytic kinetics and pseudo-first-order kinetics following an induction period.¹⁷ The latter situation may correspond to operation of different chemical mechanisms for development during the initiation and continuation stages. In this case it can be shown¹⁸ that $k = 0.25 k_{\text{auto}}[A]$, where k is the empirical rate constant as defined in Eq. 1, k_{auto} is the autocatalytic rate constant, and $[A]$ is the concentration of the non-limiting reagent, usually the developing agent in practical TDPM.

3. More recently a new model of development in TDPM has been proposed by Usanov and Kolesova, based on TEM observations on films formulated from silver stearate.¹⁹ These experiments showed that metallic silver nanoparticles form initially, not necessarily at points of contact between the silver carboxylate salt and the photocatalytic silver halide grains. Over the course of the development reaction these fine particles coagulate into larger aggregates, which are primarily responsible for the optical density. This feature of the reaction reflects Cherenov's theory of phase formation.²⁰ Stearic acid is a byproduct of the redox reaction. The melt of stearic acid, and not the silver stearate or the polymeric binder, then provides the medium in which the colloidal particles can diffuse to the reaction site during the continuation stage. In this scheme, positive feedback observable in the reaction kinetics may be attributed to the increasing volume of stearic acid available to the reaction.

Given the analogy to physical development in the proposal of KR,⁸ we can recognize certain recent examples of solution phase chemistry from the literature as potential models for the development reaction occurring in TDPM.

Nickel and co-workers¹⁸ have studied the oxidation of *p*-phenylenediamine by silver nitrate in aqueous solution. Like the development of the thermographic media reported by Shepard,² this reaction appears to be first order in both reactants. There is no induction period, however, if the medium is nucleated with sufficiently large noble metal clusters; otherwise there is an induction period that depends on the size of the nucleating clusters. The reaction rate itself, not surprisingly, depends on the number of nucleation sites that are undergoing development but not on the size of the growing silver(0) particles.

Mills and coworkers²¹ studied the base-catalyzed formation of colloidal silver in 2-propanol. In this case, the solvent is also the reducing agent; Ag_2O , formed by reaction of catalytic amounts of OH^- with silver nitrate, provides the nucleation sites. This system appeared to follow the autocatalytic rate law. The authors suggested, however, that the positive feedback was provided by an increasing

number of growing colloidal silver(0) particles over the course of the reaction, rather than, e.g., by the increasing surface area of individual particles. This system then is analogous to so-called "granular" photographic development.²² It follows from their analysis that:

1. secondary nucleation occurs in the course of the reaction and
2. that the mean particle size of the product colloid remains constant over the course of the reaction

By x-ray diffractometry, the investigators verified this second inference and showed that, under their conditions, $70 + 30 \text{ \AA}$ silver particles formed. Nickel²⁰ does not provide comparable data for his system.

The size of the particles may be controlled by thermodynamic factors, e.g., the excess surface free energy, $G(\text{surf.})_x$ of the growing particles, as given by the Gibbs-Thomson equation:

$$G(\text{surf.})_x = 2V_m/r, \quad (2)$$

where V_m is the molal volume of metallic silver, r is the particle radius, and σ is its specific surface free energy, measured to be 920 erg cm^{-2} in aqueous media.²³ Ostwald ripening of the colloidal deposit can proceed until $G(\text{surf.})_x = \text{ca. } k_b T$, i.e.,

$$r_o = 2\sigma V_m/k_b T, \quad (3)$$

which corresponds, using this estimate for σ , to ca. 60 \AA , in order-of-magnitude agreement with the observations of Huang et al.²¹ Obviously toners that can adsorb to the growing silver(0) clusters will affect σ , and, hence, the equilibrium cluster size, r_o , and, as is discussed below, the optical characteristics of the silver deposit.

Recently, Zhai and Efrima²⁴ have studied the reduction of silver ions to colloidal silver by Eriochrome Black T. The reaction is first order in silver ion when it is the limiting reagent and exhibits no positive feedback, e.g., autocatalysis. Rate of nucleation of the colloidal particles is thought to be rate determining in this case. Efrima estimates the critical diameter of the nuclei as ca. 13 \AA , corresponding to 50 to 80 silver atoms. Once this size is reached, particles may grow autocatalytically, but, as this stage of silver(0) deposition is not rate determining, it does not influence the observed kinetics.

Experimental

Materials. For these studies we used model TDPM comprising so-called preformed "full soaps," i.e., silver carboxylates precipitated in the presence of the grains of a conventionally made, ca. $0.05\text{-}\mu\text{m}$ cubic gelatino-AgBr photoemulsion. Soaps were synthesized from >95% pure stearic (C) and behenic (B) acids, as well as from a commercial (Witco Chemical Co.) blend comprising comparable amounts of stearic and behenic acids along with small amounts of acids of intermediate chain lengths⁸ (O). The soaps were dispersed in polyvinylbutyral (Sekisui BX-L) binder along with CAO-5 hindered phenolic developing agent and toners (phthalazine and 4-methyl-phthalic acid in a 2:1 ratio), with a phthalazine:Ag ratio of 0.20, comparable to that reported for typical commercial films.²⁵ These model coatings, although similar to commercial TDPM, did not contain sensitizing dye and represented a relatively low coating weight of silver (ca. 1 g Ag m^{-2}) to facilitate the experiments. Some films were also prepared using a "half soap," which comprised a 1:1 mixture of silver behenate and behenic acid in place of the full silver carboxylate.

Arrested Development Study. Samples of the full-soap films, unexposed (U) or exposed (E) to D_{\max} were developed by immersion in a Fluorinert® bath (3M FC43) thermostatted to 112° for various times to achieve predetermined levels of optical density, $0.10 \leq D \leq 0.70$, compared with typical D_{\max} levels of 1.2 to 1.5 under conditions of sensitometric exposure of the films and development to completion in a heated roller processor. The samples were then analyzed by TEM and x-ray diffractometry.

For TEM characterization, cross sections of developed films embedded in epoxy resin were cut with a glass-blade ultramicrotome to a thickness of 130 nm. These sections were imaged in a JEM-7 electron microscope with a chilled stage and accelerating voltage of 80 kV. Analysis of the TEM images is described below. Mean particle sizes of silver(0) deposits in developed films were also determined by x-ray diffractometry, with line-width analysis by the Scherrer equation.²⁶

Development Kinetics. To measure rates of development, exposed (intrinsic spectral regime) or unexposed samples were introduced into a quartz cell containing 3M Fluorinert® liquid (FC43) thermostatted at the appropriate temperature ($\pm 0.2^\circ$). We used both full-soap and half-soap films in these experiments. The cell was located in the beam of a Hewlett-Packard Model 8452 diode array UV-visible spectrophotometer with a 450-nm cutoff filter installed in the beam path to protect the sample from adventitious exposure during development. Transmission optical densities, usually at 480, 640, and 820 nm, were logged continuously after insertion of a sample into the cell. Data were accepted only from runs in which traces at each wavelength were congruent after normalization to unit optical density at completion of development.

Measurements were typically carried out over the temperature range 90 to 132°, which includes the practical development regime, as well as temperatures at which principal silver soap phase transitions are thought to occur.^{5,8} In practice, the upper limit of the temperature range of our investigations was determined by the temperature at which the induction period for development became comparable to the time required for thermal equilibration of the sample with the bath, ca. 0.2 s.

Results and Discussion

Arrested Development Study. Figures 1 and 2 show representative TEM images of exposed and unexposed TDPM at various levels of development, from micrographs originally recorded at 60,000× magnification. We observed that at all levels of development with $D \geq 0.1$ of either exposed (image) or unexposed (fog) samples, developed silver(0) particles of irregular, apparently fractal shape coexisted with spheroidal particles. On closer inspection the irregular deposits appeared to be aggregates of spheroidal particles of the same size distribution and shape as the individual ones. Aggregated and unaggregated silver particles were not uniformly distributed within the cross sections, but concentrated in domains of ca. 3- μm length parallel to the film plane and $\leq 1 \mu\text{m}$ in the normal direction. These dimensions correspond approximately to those of silver carboxylate micelles visible in TEM images of undeveloped samples.

We counted and measured sizes of unaggregated spheroids and readily resolvable spheroidal components of aggregates visible in the 60,000× micrographs. These data are given in Table I:

1. D indicates the developed transmission optical density of the sample,
2. n_{Ag} is the number of spheroids counted in a ca. 15- μm^2 cross-sectional area of the film (ca. 2- μm^3 sample volume),

TABLE I. Developed Silver(0) Particle Size Analysis by TEM and by X-Ray Diffractometry

Sample	D	n_{Ag}	$d(\text{TEM})$ (Å)	$d(\text{x-ray})$ (Å)
C(Exp.)	0.76	24	(430 \pm 140)	188
	0.53	22	(400 \pm 100)	181
	0.72	28	(420 \pm 127)	184
	0.30	31	(460 \pm 100)	202
	Avg.	26.2	(427 \pm 21.5)	(187 \pm 8.3)
C(Unexp.)	0.58	19	(325 \pm 100)	220
	0.31	32	(345 \pm 132)	137
	0.35	61	(400 \pm 137)	139
	0.56	39	(392 \pm 125)	160
	0.45	31	(413 \pm 102)	151
	Avg.	36.4	(375 \pm 34)	(161 \pm 30)
B(Exp)	0.49	—	—	195
	0.38	29	(508 \pm 148)	196
	0.10	21	(460 \pm 110)	133
	0.11	17	(505 \pm 120)	222
	Avg.	22.3	(490 \pm 22)	(186 \pm 33)
B(Unexp.)	0.50	62	(412 \pm 122)	175
	0.36	66	(404 \pm 151)	180
	0.27	53	(467 \pm 200)	158
	0.15	45	(450 \pm 130)	227
	0.08	—	—	204
	Avg.	56.5	(433 \pm 26)	(188 \pm 24)
O(Exp.)	0.66	27	(454 \pm 162)	209
	0.62	31	—	213
	0.40	54	(438 \pm 119)	195
	0.25	112(?)	(438 \pm 128)	246
	Avg.	56	(443 \pm 7.5)	(215 \pm 18)
O(Unexp.)	0.34	147	(404 \pm 121)	130
	0.23	90	(387 \pm 121)	142
	0.10	36	(437 \pm 116)	188
	Avg.	91	(409 \pm 21)	(153 \pm 25)
Overall mean	(0.38 \pm .19)	(48 \pm 31)	(421 \pm 44)	(182 \pm 31)
Contrasts for effect of:				
Soap*	-0.12	+4.0	+30.2	+0.66
Exposure	-0.04	-13.2	+23.7	+14.4
Conf. Limit	± 0.043	± 6.9	± 9.8	± 6.9
(\pm one standard error of overall mean)				
Analyses of regression of D on...				
r	—	-0.291	-0.377	+0.135

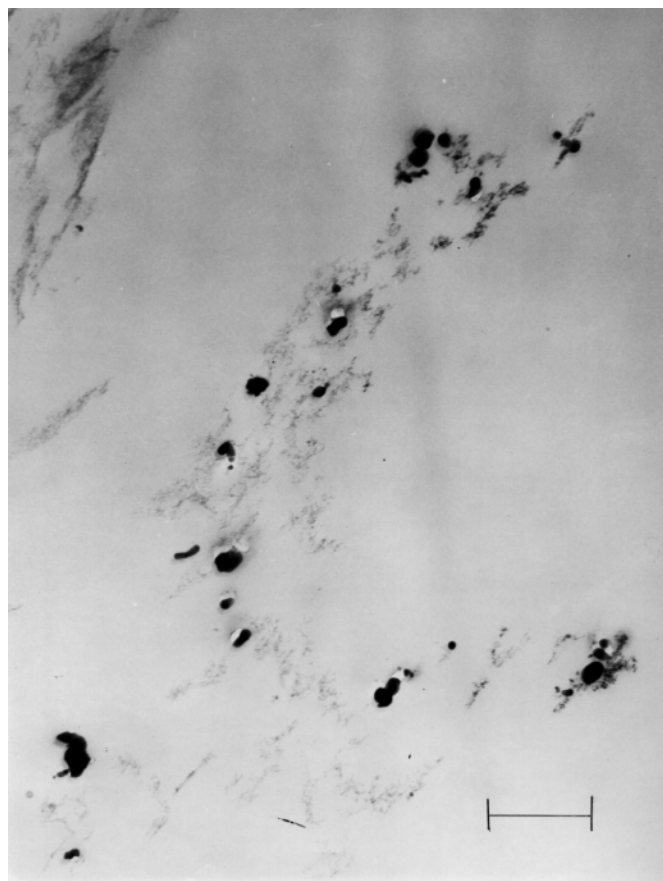
* For analysis of design, soap C = -, B = +, O = 0.

3. $d(\text{TEM})$ is the mean spheroid diameter (± 1 std. deviation); and

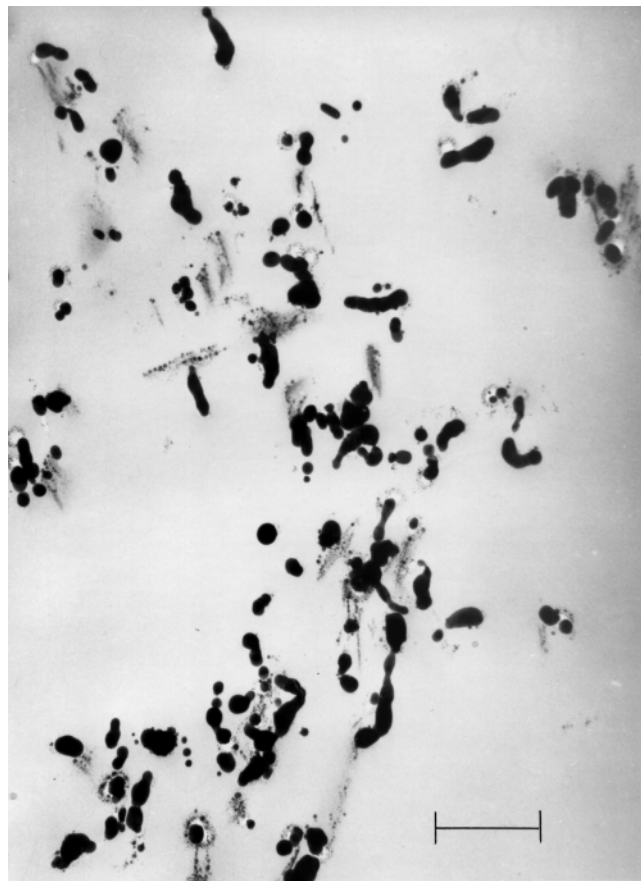
4. $d(\text{x-ray})$ is the corresponding estimate from x-ray diffractometry on the same samples.

The TEM estimates are approximately twice the x-ray diffraction estimates, which may reflect the dendritic character of even unaggregated spheroids, observable at still higher TEM magnification, e.g., 120,000×. The possibility that the apparently spheroidal particles may be fractal solids can rationalize the fact that experimentally observed dimensions are large compared with the prediction of Eq. 3. Keep in mind that only unaggregated spheroids were counted to estimate $d(\text{TEM})$ but $d(\text{x-ray})$ is an average of monocrystalline domains in all the deposited silver(0).

Regression analyses for $d(\text{TEM})$ or $d(\text{x-ray})$ on D over the entire range of densities yielded correlation coefficients, r , which were not significant at even the 90% confidence level. Thus the size of the monocrystalline domains in developed particles does not change with degree of development, and increasing optical density and increasing mass of developed silver(0) with time of development correspond



(a)

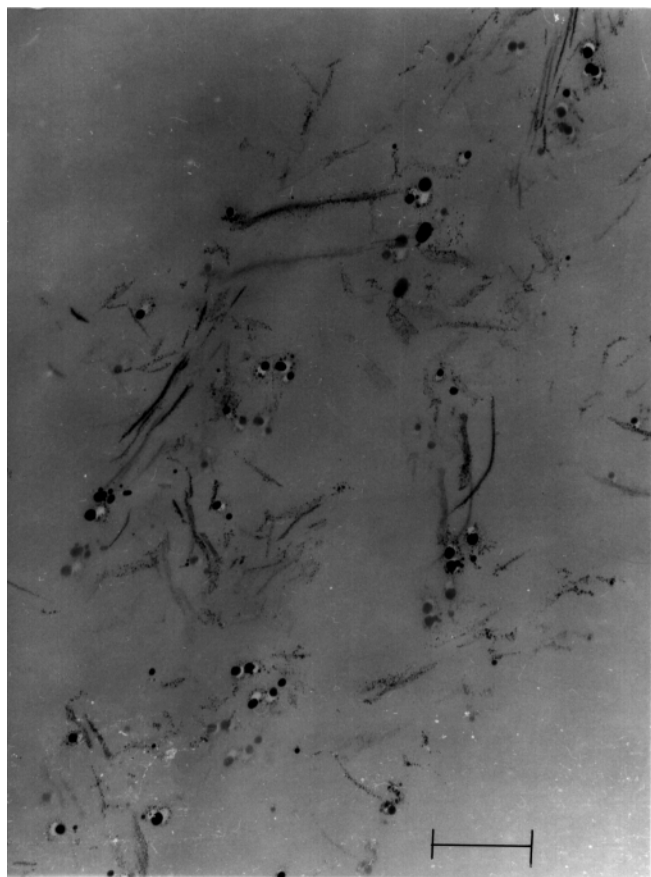


(b)

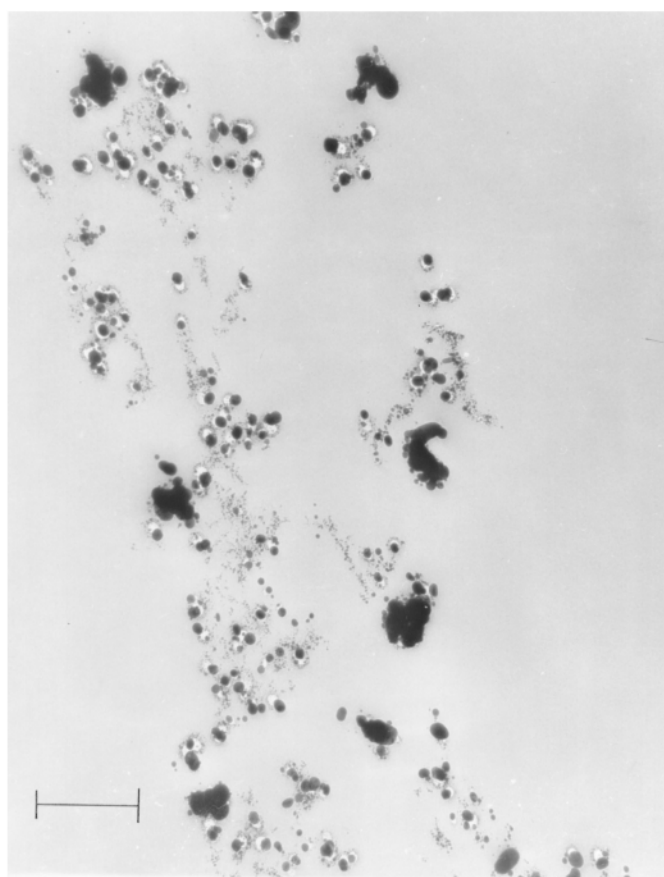
Figure 1. TEM images of cross sections of light-exposed TDPM thermally developed to (a) $D = 0.15$, (b) $D = 0.30$, and (c) $D = 0.53$. Scale bar corresponds to $0.5\ \mu\text{m}$.



(c)



(a)



(b)

Figure 2. As Figure 1, unexposed TDPM developed to (a) $D = 0.10$, (b) $D = 0.23$, and (c) $D = 0.35$.



(c)

to an increasing number of developed silver(0) particles, as in Mills' solution-based system.²¹

Analysis of the data of Table I as a factorial design revealed that in unexposed films, e.g., Fig. 2, fog aggregates were smaller, and that unaggregated spheroidal particles were both smaller and more numerous. In both exposed and unexposed examples the unaggregated spheroids represented ca. 6% of the theoretically developable silver in each section. Apparent invariance of n_{Ag} with D above this threshold suggests that this population represents a steady-state concentration of unaggregated spheroidal particles, which is established during the initiation stage and is maintained during the continuation stage of the development reaction.

Aggregation implies that these silver(0) spheroids must be mobile in the reaction medium, which has been proposed to be the free fatty acid byproduct of development.¹⁹ We would expect the time required for their aggregation, t_{agg} , to be given by $x^2/2D$, where x is the mean diffusion distance, taken as comparable to the linear dimension of the sphere of influence, 0.2 μm (see below), and D is the diffusion coefficient for spheres of radius $r = 200 \text{ \AA}$ according to the Stokes–Einstein relationship:

$$D = k_b T / 6r\eta. \quad (4)$$

The rheology of melts of C_{12} – C_{18} fatty acids has been characterized by two groups whose data are in good agreement,²⁷ and viscosity, η , was found to obey the Andrade equation,²⁸ so that for a C_n acid

$$\ln \eta = [(0.16 + 0.0042 n) / k_b T] - 5.57, \quad (5)$$

which yields for behenic acid (C_{22}) at 120° , $\eta = (5.9 \pm .2) \text{ cP}$, i.e., $0.06 \text{ erg s cm}^{-2}$. Substituting this estimate into Eq. 4 yields $D = 2 \times 10^{-11} \text{ cm}^2 \text{ s}^{-1}$ and $t_{agg} = 10 \text{ s}$, comparable to typical development times for TDPM.

The number of AgBr grains, n_{AgBr} , capable of photocatalytic generation of latent image centers in one TEM image section in this experiment is

$$n_{AgBr} = 188 f_{AgBr} c_{Ag} V_o / V_{grain} \rho, \quad (6)$$

where c_{Ag} is the molar silver concentration in the dry coating ($3.5 \times 10^{-3} \text{ mol cm}^{-3}$), f_{AgBr} is the mol fraction of silver present as AgBr (0.025), V_o is the section volume, taken as the product of the image area and the TEM depth of focus (assumed to be an upper limiting value of 0.05 μm), V_{grain} is the average AgBr grain volume ($1.25 \times 10^{-16} \text{ cm}^3$ based on the TEM observations), and ρ is the density of AgBr (6.5 g cm^{-3}). Assuming a Poisson distribution of grains among TEM image frames, we estimate $n_{AgBr} = (16 \pm 4) \text{ grains/image}$.

In the actual TEM images we observed appreciable aggregation of AgBr grains; they occurred typically in clumps of 2 to 3, sometimes more. On sections of undeveloped model film we typically found 20 to 25 AgBr grains, in reasonable agreement with the theoretical estimate. On images of developed material we could not distinguish AgBr grains from the silver(0) particles, which also tended to be ca. 400 \AA in diameter (by TEM).

Long-chain silver carboxylates and polyvinylbutyral are mutually insoluble. TEM images of undeveloped photothermographic films typically revealed two phases, identified as silver carboxylate and polyvinylbutyral, apparently without appreciable intermixing. By DSC analysis of such representative films, phase transitions characteristic of the pure silver carboxylates²⁹ and the glass transition of polyvinylbutyral were clearly distin-

guishable, which supports our interpretation of these images. X-ray diffractometry of the films also revealed the normal reflections assigned to pure silver carboxylates.

In the TEM cross sections the silver carboxylate phase, incorporating the AgBr grains, accounted for on average 12% of the image area, designated f_{AgBeh} . Thus we can estimate the radius, r , of the sphere of influence of one AgBr grain for development to completion as

$$r = (f_{AgBeh} a / \pi n_{AgBr})^{0.5}, \quad (7)$$

where a is the TEM section area ($1.65 \times 10^{-7} \text{ cm}^2$ at $60,000\times$ magnification). Equation 7 yields $r = 0.2 \mu\text{m}$, in good agreement with other estimates of this parameter.^{8,18} We should point out that the volumes within the silver carboxylate phase observed in the TEM images to be depleted of silver on complete development tend to be quite irregular in shape, not actually spheres at all. Their morphology appears to be determined rather by morphological features of individual silver carboxylate micelles.

Incorporation of all silver from one such sphere of influence, i.e., complete development, into ca. 400- \AA spheroids requires 33 such silver(0) particles per sphere of influence (n_{Ag}/n_{AgBr}). At optical densities below onset of aggregation, the number of silver(0) spheroids, n_{Ag} , observable in TEM images correlated linearly with transmission optical density, with $r = 0.998$.

$$n_{Ag} = 442.4 D - 2.5. \quad (8)$$

Extrapolation to $D_{max} = 1.4$ for the model film yields 612 individual, monocrystalline silver particles; so $n_{Ag}/n_{AgBr} = 38$. If each individual silver(0) deposit requires a unique nucleation event, n_{Ag}/n_{AgBr} is the number of spatially random nucleation events occurring in one sphere of influence. The two estimates of this parameter are in good agreement, and they support the hypothesis of secondary nucleation. No specific mechanism of secondary nucleation in the development of TDPM has been confirmed experimentally, however; possibilities include:

1. infectious development;
2. stress-wave propagation,^{30a} which creates new defect sites on the silver carboxylate particle undergoing development; and
3. fragmentation of a dendritic silver(0) deposit, with the fragments diffusing through the fatty acid melt to new sites to become growth nuclei.

An alternative rationale would be that photocatalysis by AgBr grains extends to sites remote from the AgBr grain. This latter proposal is difficult to rationalize mechanistically. On the other hand, secondary nucleation is commonplace in heterogeneous reactions, and a variety of mechanisms have been proposed.³⁰ We believe that it is important to relate the involvement of secondary nucleation of silver carboxylate development to the observation of Usanov and Kolesova,¹⁹ namely, that development can be initiated at sites on the silver carboxylate micelle that are not in contact with a silver halide grain.

Development Kinetics. A typical trace from the real-time probing of TDPM development is shown in Fig. 3; analysis of the data according to Eq. 1 is also illustrated. We estimated t_i by extrapolation of the linear portion of the experimental trace to D_o , the undeveloped optical density of the sample. Thus only one parameter in Eq. 1 had to be adjusted to obtain the fit shown. As expected, fits of our experimental traces to the autocatalytic rate law were equally valid statistically; presumably other two-parameter kinetic forms are also

TABLE II. Arrhenius Activation Parameters for Development of TDPM

	A_i	E_i^a	A_c	E_c^a
Full soap:				
Image (B)	55.4	1.98 eV	55.3	1.93 eV
Image (C)	53.0	1.75	54.1	1.89
Image (O)	51.8	1.64	53.0	1.83
Image (avg.)	(53.4 ± 1.5)	(1.79 ± 0.14)	(54.1 ± 0.9)	(1.88 ± 0.04)
Fog (avg.)	(46.1 ± 1.6)	(1.7 ± 0.2)	(53.1 ± 1.4)	(1.74 ± 0.15)
Half soap:				
Image	65.6	(2.2 ± 0.2)	52.0	(1.8 ± 0.2)
fog	36.9	1.30	51.8	(1.8 ± 0.2)

applicable. Use of Eq. 1 is, however, consistent with both the early studies on silver-based thermographic media² and Nickel's model system.¹⁸

Plots according to the Arrhenius equation

$$k = A_c \exp(-E_c^a/k_b T), \quad (9a)$$

$$1/t_i = A_i \exp(-E_i^a/k_b T), \quad (9b)$$

of the k and $1/t_i$ data over the temperature range from 90 to 132° were generally linear and yielded the activation parameters reported in Table II. No statistically significant differences were found among the B, C, and O series samples. The monotonic trends in both k and $1/t_i$ over the temperature regime where significant phase transitions are known to occur in silver carboxylates^{5,8,29} are incompatible with models of development of TDPM in which such phase transitions are suggested to play a role.

From the A parameters we infer large, positive entropies of activation, typically of the order of 400 to 450 J K⁻¹ mol⁻¹. These values are consistent with the dissociation of coordination complexes, as proposed by Whitcomb and coworkers,³¹ occurring in concert with one-electron reduction of complexed silver ion, in the rate-determining step of the development reaction. It is also apparent that for the full-soap systems, selectivity of development, i.e., the ability to discriminate levels of exposure during development, is reflected exclusively in the preexponential parameter for t_i . Exposure history thus affects the entropy of activation for the thermographic reaction during initiation of development. In this regard, development of TDPM differs from conventional photographic development: in the conventional system, selectivity of development may be reflected in E^a as well.³²

For the TDPM the large values of E^a in all cases suggest furthermore that kinetics in neither stage of the reaction are likely to be mass transport limited. Rather, we draw the following three inferences from the data of Table II:

1. The activation energies specifically suggest a continuity of mechanism of reaction encompassing both the initiation stage, occurring during t_i , and the continuation stage, for light-exposed full-soap films.
2. The data likewise suggest a mechanistic discontinuity for the exposed half-soap films.
3. The activation energies obtained for t_i of the unexposed films presumably reflect E^a for the as-yet mechanistically unspecified process of fog center nucleation. (One of the reviewers of this report points out that, from the data of Table II, the mechanisms of fog formation in full-soap and half-soap TDPM must accordingly differ).

To account for these results we propose a two-step model of the thermography reaction:

1. Silver ion complexing reagents (L), e.g., phthalazine and 4-methylphthalic acid in our case, react with silver ion from the silver carboxylate^{8,31} to form com-

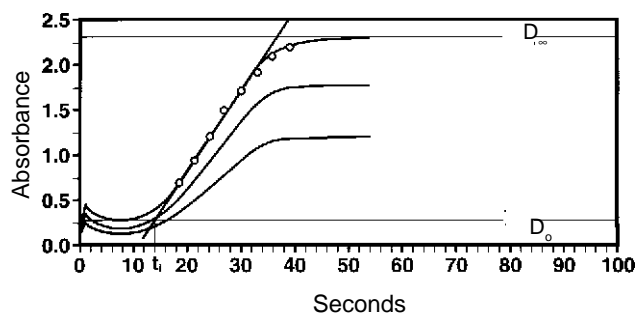
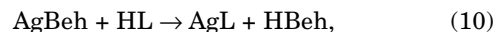


Figure 3. Representative kinetic traces for development of TDPM in thermostatted fluorochemical liquid bath, showing geometrical method for estimation of t_i ; curves recorded (top-to-bottom) at 480, 640, and 820 nm. Data points correspond to fit of data to Eq. 1.

plexes that dissolve in the fatty acid melt and diffuse therein to the reactive sites, at which

2. they are reduced to elemental silver by interaction with the developing agent (D) at these sites, which may be growing elemental silver particles, Ag_n^o.

This model can be expressed as the following reaction sequence:



for which we further assume that the number of accessible nucleation sites, whether latent image or secondary nuclei (see above), is proportional to the reaction volume, i.e., the volume of free fatty acid, V_{HBeh} . This assumption accommodates the role of byproduct carboxylic acid proposed by Usanov and Kolesova.¹⁹

Reaction according to Eqs. 10 and 11 with this assumption can be expressed in the following series of differential equations:

$$-d[\text{L}]/dt = d[\text{AgL}]/dt = k_9[\text{L}]a_{\text{AgBeh}} - k_{10}[\text{AgL}][\text{D}]V_{\text{HBeh}}, \quad (12)$$

$$dV_{\text{HBeh}}/dt = k_9[\text{L}]a_{\text{AgBeh}}, \quad (13)$$

$$dm/dt = (1/q)k_{10}[\text{AgL}][\text{D}]V_{\text{HBeh}}, \quad (14a)$$

or

$$d(mq)/dt = k_{10}[\text{AgL}][\text{D}]V_{\text{HBeh}}. \quad (14b)$$

Accordingly Eq. 14b expresses the rate of increase in number of image-forming silver clusters. We take this response as approximately linear with measurable optical density, insofar as the clusters grow to some limiting size, of index q , which is time invariant, as already demonstrated in the arrested development study.

The system of (Eqs. 12, 13, and 14) was integrated numerically, with further assumptions that the activity of solid silver carboxylate, a_{AgBeh} , and the concentration of developing agent, $[\text{D}]$, which is present in excess in our experimental examples, were both unity. V_{HBeh} was expressed as the fractional degree of conversion of silver carboxylate to free carboxylic acid. We formulated the rate constants k_{10} and k_{11} for Eqs. 10 and 11, respectively, in Arrhenius form with $E^a = 2.7$ eV for Eq. 10 and 1.35 eV for Eq. 11. Values of these rate constants are given in Table III. Initial values of V_{HBeh} were allowed to vary from 0.001 (full soap) to 0.5 (half soap). The simulated kinetic data corresponded to Eq. 1. The activation energies derived thereby are given in Table III.

TABLE III. Computer-Simulated Kinetics of TDPM Development

Rate constants (for all values of V_{HBeh})			
$T(^{\circ}\text{C})$	k_{10}	k_{11}	k
110	0.030 s ⁻¹	0.0175 s ⁻¹	0.018 s ⁻¹
115	0.087	0.030	0.039
120	0.245	0.050	0.079
125	0.66	0.081	0.162
130	1.75	0.133	0.33
ΔE^a	2.55	1.26	1.81 eV
Activation energies:			
V_{HBeh}	ΔE^a	ΔE^b	
0.001 (full soap)	1.25 eV	1.78 eV	
0.01	1.38	1.88	
0.10	1.42	1.78	
0.25	1.52	1.73	
0.50 (half soap)	(2.4 ± 0.1)	1.74	
Avg.	—	(1.78 ± 0.055) eV	

* Molar ratio of free fatty acid to silver carboxylate.

It is clear that this model accommodates the differences in behavior between the full-soap and half-soap systems, expected for the proposed¹⁹ role of free carboxylic acid in the thermal development scheme. Accordingly the higher activation energy, E_a^* , for half-soap TDPM indicates that the rate of development during the initiation phase is limited by the rate of formation of the intermediate silver(I) complex under these conditions. However, when smaller levels of free fatty acid are present initially, the redox reaction is rate limiting throughout the course of development.


Conclusions

Major conclusions from the arrested development study are as follows:

1. During the initiation stage of development small, spheroidal silver(0) particles form,
2. Over the course of the development reaction, the number of silver(0) spheroids increases, but not their average size,
3. This process requires secondary nucleation of the silver(0) phase-forming reaction by an as-yet unestablished mechanism,
4. Above some threshold concentration, whose establishment corresponds to the onset of the continuation stage of development, these spheroids aggregate to form the light-absorbing species comprising the TDPM image.

We arrived at these principal conclusions from development kinetics studies on TDPM:

1. Image-background discrimination is the result of an exposure-level dependence of the entropy of activation during the initiation stage of the development reaction,
2. There is no discontinuity of mechanism at the molecular level between the initiation and continuation stages of development with full-soap TDPM,
3. Silver ion complexing agents are involved in the rate-determining step of development of TDPM, as proposed by KR⁸ and Whitcomb.³¹
4. Differences in behavior between half-soap and full-soap TDPM support the proposal that liberation of free fatty acid provides the positive feedback for the development reaction.

The simple chemical scheme of Eqs. 10 and 11 thus embodies a system of reactions that incorporates the basic features of the development reaction of TDPM, including temperature dependence and differences between full and half soaps. 

Acknowledgment. We thank Dr. Myles Brostrom (3M Analytical and Properties Research Laboratory) for the

x-ray diffraction analyses, and Dr. T. J. LePage (present address: Dept. of Chemistry, University of California, Irvine, CA) for the DSC analyses. We thank many colleagues, especially Drs. Lilia Burleva and Anatoly Sidelnikov, Institute for Solid State Chemistry, Akademgorodok, Novosibirsk, Russia, for helpful discussions. We also thank Mr. Jan Alboszt, 3M International, for his facilitation of international communication and cooperation, and Dr. G. C. Nicholson, vice-president, 3M International Laboratory Operations, for support of this work.

References

1. W. H. Fox Talbot, US Patent 5,171 (1847).
2. J. W. Shepard, *J. Appl. Photogr. Eng.* **8**: 210 (1982).
3. D. P. Sorensen and J. W. Shepard, US Patent 3,152,904 (1964).
4. B. L. Shely and J. W. Shepard, US Patent 3,429,406 (1969).
5. M. Ikeda, *Photogr. Sci. Eng.* **24**: 273, 277 (1982).
6. T. Kokubo, T. Aizu, and S. Nishiyama, in *Paper Summaries, SPSE 35th Annual Conference*, SPSE, Washington, DC, 1982, paper M-3.
7. D. A. Morgan, *Proc. SPIE* **1253**: 239 (1990).
8. D. H. Klosterboer, in *Imaging Materials and Processes, Neblette's 8th ed.*, J. M. Sturge, V. Walworth and A. Shepp, Eds., Van Nostrand-Reinhold, New York, 1989, chap. 9.
9. V. M. Andreev, L. P. Burleva, V. V. Boldyrev, and Yu. I. Mikhailov, *Isv. Sib. Otd. Akad. Nauk. SSSR, Ser. Khim. Nauk.* **4**(2): 58 (1983); V. M. Andreev, L. P. Burleva, and V. V. Boldyrev, *ibid.* **5**(5): 3 (1984); L. P. Burleva, V. M. Andreev, and V. V. Boldyrev, *J. Thermal Anal.* **33**: 735 (1988).
10. (a) S. E. Shepard and W. Vanselow, US Patent 1,976,302 (1934); (b) S. Suchow and S. H. Herah, US Patent 2,700,610 (1955).
11. W. Ostwald, *Lehrbuch der allgemeinen Chemie*, Vol. 2, part 1, 2nd rev. ed., Englemann, Leipzig, 1910, p. 1078; R. Abegg, *Ann. Phys. Chem.* **62**: 425 (1897); R. Abegg, *Arch. Wiss. Phot.* **1**: 15, 109 (1899); K. Schaum, *ibid.* **1**: 139 (1899).
12. T. H. James, in *The Theory of the Photographic Process*, 4th ed., Macmillan, New York, 1977, chap. 13.
13. D. H. Klosterboer and R. L. Rutledge, in *Paper Summaries, SPSE 33rd Annual Conference*, SPSE, Washington, DC, 1980, paper N-7.
14. (a) T. H. James, *J. Am. Chem. Soc.* **61**: 648, 2379 (1939); *J. Phys. Chem.* **45**: 223 (1941); (b) R. B. Pontius, R. M. Coles and R. J. Newmiller, *Photogr. Sci. Eng.* **4**: 123 (1960); (c) G. I. P. Levenson and P. J. Twist, *J. Photogr. Sci.* **21**: 211 (1973); **22**: 169 (1974); (d) M. R. V. Sahyun, *Electrochim. Acta* **23**: 1145 (1978).
15. M. R. V. Sahyun, *Photogr. Sci. Eng.* **18**: 504 (1974).
16. C. Zou, M. R. V. Sahyun, B. Levy, and N. Serpone, *J. Imaging Sci. Technol.*, **40**: 94 (1996).
17. K. R. C. Gisser, in *Paper Summaries, IS&T's 49th Annual Conference*, IS&T, Springfield, VA, 1996, paper IIIB-6.
18. U. Nickel, N. Rühl and B. M. Zhou, *Z. Phys. Chem.* **NF148**: 33 (1986).
19. Yu. E. Usanov and T. B. Kolesova, *J. Imaging Sci.*, **40**: 104 (1996).
20. S. F. Cherenov, Yu. V. Fedorov and V. N. Zakharov, *J. Infor. Rec. Mater.* **19**: 291 (1991); S. F. Cherenov, E. A. Galashin and Yu. V. Fedorov, *ibid.* **18**: 107 (1990).
21. Z.-Y. Huang, G. Mills and B. Hajek, *J. Phys. Chem.* **97**: 11542 (1993).
22. (a) T. H. James, in *The Theory of the Photographic Process*, 3rd ed., Macmillan, New York, 1966, p. 352; (b) M. R. V. Sahyun, *Photogr. Sci. Eng.* **19**: 38 (1975); (c) T. Tani, *J. Imaging Sci.* **39**: 355 (1995) and references cited therein.
23. J. Malinowski, in *Growth and Properties of Metal Clusters*, J. Bourdon, Ed., Elsevier, Amsterdam, 1980, pp. 303ff and references cited therein.
24. X. Zhai and S. Efrima, *J. Phys. Chem.* **100**: 1779 (1996).
25. (a) M. Simons, US Patent 3,839,049 (1972); (b) J. M. Winslow and I. R. Maw, US Patent 4,161,408 (1979); (c) H. W. Altland and D. D. F. Shiao, US Patent 4,351,896 (1982).
26. H. P. Klug and L. E. Alexander, *X-Ray Diffraction Procedures*, Wiley, New York, 1954.
27. (a) H. Nouredini, B. C. Tesh, and L. D. Clements, *J. Am. Oil Chem. Soc.* **69**: 1189 (1992); (b) F. Fernandez-Martin and F. Montes, *ibid.* **53**: 130 (1976).
28. E. N. da C. Andrade, *Nature* **125**: 309 (1930).
29. M. Ikeda, *Photogr. Sci. Eng.* **24**: 277 (1980); M. Ikeda and Y. Iwata, *ibid.* **24**: 273 (1980).
30. (a) T. Luty and C. J. Eckhardt, *J. Am. Chem. Soc.* **117**: 2441 (1995); (b) E. V. Boldyeva, *Reactivity of Solids* **8**: 269 (1990); *J. Thermal Analysis* **38**: 89 (1993); (c) V. V. Boldyrev, *ibid.* **40**: 1041 (1993).
31. D. R. Whitcomb, W. C. Frank, R. D. Rogers, B. P. Tolochko, S. V. Chernov, and S. G. Nikitenko, *J. Imaging Sci. Technol.*, in press.
32. T. H. James, in *The Theory of the Photographic Process*, 3rd ed., T. H. James, Ed., Macmillan, New York, 1966, Chap. 16 and references cited therein.